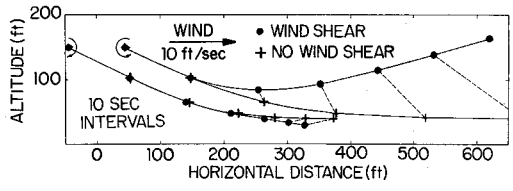

Fig. 4 Calculated vortex trajectories in the ground frame of reference.

B-727 aircraft. In the frame of reference moving with the wind, the wind shear vortices normally move at half the wind speed in the direction opposite to the wind (i.e., 5 fps to the left in Fig. 3). The effect of the aircraft vortices on this motion is to speed it up on the up-wind side and to reverse it on the down-wind side. The wind shear vortices approaching from the right in Fig. 3 are swept up in the air and eventually induce the down-wind vortex to reverse its downward motion and move back up. After 60 sec, this vortex has captured wind shear vorticity of equal magnitude to its own and is moving upward at a speed comparable to its initial downward motion. The up-wind vortex, on the contrary, finds itself isolated from wind shear vorticity and therefore is influenced only by its image vortex. These motions are shown in Fig. 4 in the ground frame of reference. For comparison, the trajectories for a uniform wind are also shown. The trajectory of the up wind vortex is almost the same for the two cases, as one might expect.

Although the model used here is crude, it gives a qualitative description of the observed difference in the motion of the two vortices. The effect is similar to but stronger than that proposed by Harvey and Perry[1] to explain the rising of vortices. It should be noted that the effect discussed in this note is actually produced by the vertical gradient in the wind shear rather than by the wind shear directly. One can easily see that the wind shear vortices would not affect the aircraft vortex vertical motion at all if they were uniformly distributed in space.

The phenomenon described in this Note pertains to relatively low cross winds. Both experimental observations and calculations indicate that other phenomena occur at much higher cross wind speeds (e.g. 30 fps instead of the 10 fps considered here).

Reference

[1] Harvey, J. K. and Perry, F. J., "Flowfield Produced by Trailing Vortices in the Vicinity of the Ground," *AIAA Journal*, Vol. 9, No. 8, Aug. 1971, pp. 1659–1660.

Three-Dimensional Structure and Equivalence Rule of Transonic Flows

H. K. Cheng* and Mohammed Hafez†
University of Southern California, Los Angeles, Calif.

Introduction

For smooth configurations of very low aspect ratio, a theoretical basis of Whitcomb's transonic area rule[1] has been established by Oswatish and Keune[2] and Guderley[3] for the nonlifting case, and by Cole and Messiter[4] and Ashley and Landahl[5] for the more general case with lift. Basic to the cited works[2–5] is a field structure composed of two distinct regions: an inner region similar to that in the classical slender-body (Jones/Ward/Adams and Sears) theory,[6–8] and an axisymmetric outer region governed by the transonic smalldisturbance equation. The same field model has been employed recently by Stahara and Spreiter[9] in which configurations of unit-order aspect ratio were considered.

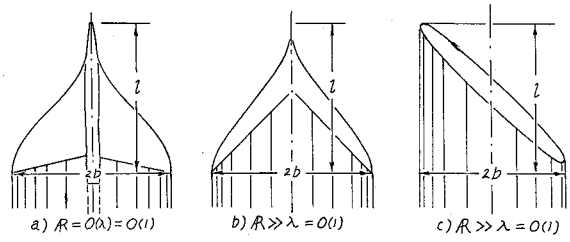

Fig. 1 Examples of configurations studied.

This Note is concerned with the basic structure of three-dimensional transonic flows around configurations having finite (nonvanishing) leading-edge sweep angles. Refer to Fig. 1 for examples. We should like to point out that, unlike the field model stipulated in Refs. 2–5 and 9, the inviscid transonic small-disturbance regime admits three domains, representing different degrees of asymmetry controlled by the lift. Only in the domain where the lift contribution is relatively small will the area rule be applicable and, even in this case, its corrections are not all together negligible.

Basic to the present study are the parameters λ, τ, and α characterizing, respectively, the leading-edge angle of the planform, the configuration thickness ratio, and a degree of asymmetry associated with the lift or the side force. For the class of configurations of interest, these parameters may be defined as

$$\lambda \equiv b/l, \quad \tau \equiv S_{\max}/bl, \quad \alpha \equiv F_{\max}/\rho_\infty U_\infty^2 b^2 \tag{1}$$

where b is the half span, and l an over all length, $S_{\max}$ the maximum cross-sectional area and $F_{\max}$ the maximum integrated lateral force. For a Concorde-type planform, such as that of a in Fig. 1, λ is comparable to the classical aspect ratio $AR \equiv 4b^2/$(planform area). On the other hand, for a swept or yawed wing of high aspect ratio, such as that of b or c in Fig. 1, λ will be very much smaller than AR. Note that τ and α give the thickness ratio and incidence for the configuration as a whole and may be much smaller than the corresponding values characterizing a local wing section. The frame work of our analysis is then defined by

$$|M_\infty - 1| \ll 1, \quad \tau \ll 1, \quad \alpha \ll 1, \quad \lambda = 0(1) \tag{2}$$

So long as $\lambda = 0(1)$, the theory admits low as well as high aspect ratio wings. We assume in the following a steady flow of a calorically perfect gas with a uniform freestream. The perturbation field in this problem can be described by a potential, subject to a relative error comparable to the square of the perturbation velocity.

The Inner flow Region

Let x, y, and z be the Cartesian coordinates with the x axis running parallel to the freestream (occasionally, we may refer y as x_2, and z as x_3). To render the analysis more definite, the solution for the perturbation velocity potential will be written in ascending order of τ and α as (for the inner region)

$$\varphi/Ub = \tau \cdot \ln\varepsilon \cdot g(x) + \tau\varphi_\tau + \alpha\varphi_\alpha + \dots \tag{3}$$

where the logarithm of a small parameter ε is anticipated to arise from the matching with the outer solution and will be determined in the course of the analysis. The set of reduced variables which will remain at unit order in the inner region consists of $\tilde{x} = x/l$, $\tilde{y} = y/b$, $\tilde{z} = z/b$, g, φ_τ, φ_α, $\tilde{S} = S/\tau bl$ and $\tilde{f}_j = F_j/\alpha\rho_\infty U^2 b^2$, with $j = 2$ or 3. In terms of these reduced variables, the partial differential equation governing the inner

Received March 6, 1972; revision received March 28, 1972. The work is supported by the Office of Naval Research, Contract N00016-67-A-0269-0021.

Index categories: Aerodynamic and Powerplant Noise (Including Sonic Boom); Aircraft Configuration Design.

* Professor, Division of Engineering and Applied Mechanics. Member AIAA.

† Research Assistant, Division of Engineering and Applied Mechanics.

solution can be simplified under the condition of Eq. (2), dropping tildas, to

$$[(\partial^2/\partial y^2) + (\partial^2/\partial z^2)](\varphi_\tau, \varphi_\alpha) = 0 \tag{4}$$

for an arbitrary $g(x)$. The solutions sought are finite and acyclic, uniquely determined by the impermeable body surface condition and the vanishing of the transverse velocity at $r^2 \equiv y^2 + z^2 \to \infty$. The remainder in φ_τ and φ_α so determined can be estimated from the contribution of the nonlinear and linear terms omitted from Eq. (4) to be at most (for $r \neq \infty$)

$$R = 0\{(\tau \ln \varepsilon + \alpha)[(\tau \ln \varepsilon + \alpha)\lambda + |M_\infty - 1|]\lambda^2\} \tag{5}$$

The point of departure of the subsequent development is given by the behavior of φ/Ub at large r, which may be written, after making use of the body surface condition, as

$$\varphi/Ub \sim \tau \ln \varepsilon g(x) + \tau C_1(x) + \tau(S'(x)/2\pi) \ln r + (\tfrac{1}{2}\pi)[\alpha f_j(x) - \tau(d/dx)(\bar{x}_j S)]l_j(\omega)/r \tag{6}$$

where $l_j(\omega)$ are $\cos\omega$ and $\sin\omega$ for $j = 2$ and 3, respectively, $\bar{x}_j$'s are the coordinates of the cross-sectional centroid in the transverse plane (divided by b), and the repeated index j signifies summation over $j = 2$ and 3. The third and fourth terms on the right hand side of Eq. (6) give the equivalent source and doublet distributions; the latters' strengths are completely determined as in the slender-body theory once the configuration geometry is specified. Equation (6), hence also the linear inner solution itself, fails as a valid approximation for an unbounded r, as will be presently shown. It is expedient to point out at this juncture that subsequent matching of the inner and outer solutions will confirm the relations

$$g(x) = S'(x)/2\pi, \quad \varepsilon = b/b' \tag{7}$$

where b' is the proper length scale for y and z of the outer region. The relations in Eq. (7) are in fact the same as those in the subsonic and supersonic slender-body theories.[5-7]

Nonlinear Outer Region: Three Domains

The fuller equation governing the perturbation potential, without nondimensionalization, is

$$\varphi_{yy} + \varphi_{zz} = [(M_\infty^2 - 1) + (\gamma + 1)M_\infty^2\varphi_x/U]\varphi_{xx} + O(\varphi_x\varphi_{yy}/U, \text{etc.}) \tag{8}$$

The group of nonlinear terms not fully written out belong to an order φ_x/U higher than the terms on the left. The first two terms on the right cannot be neglected at large r and are the principal ingredients of the transonic small-disturbance theory. Consider first the situation wherein the outer limit Eq. (6) is dominated by the thickness, or at least the thickness is as important as the lift and side forces. This requires $\alpha = O[\tau r \ln(\varepsilon r)]$ or smaller, anticipating the universal forms of $g(x)$ and ε. We may then estimate φ from Eq. (6) at large r as $\varphi/Ub = O[\tau \ln(\varepsilon r)]$. With this, we may then estimate the size of the two terms associated with φ_{xx} in Eq. (8) for large r, and arrive after quadrature at the error estimate for the inner solution to φ/Ub at large r:

$$R = O[(M_\infty^2 - 1)\tau\lambda^2 r^2 + (\gamma + 1)M_\infty^2\tau^2\lambda^3 \ln^2(\varepsilon r)] \tag{9}$$

Comparing R with φ/Ub, and recalling $\varepsilon = b/b'$, we identify the region of nonuniformity of the inner solution (which is to be the nonlinear transonic region) at

$$r = 0(b'/b) = 0[(1/\tau\lambda^3)^{1/2}] \tag{10}$$

where $\varphi/Ub = 0(\tau)$, provided

$$K \equiv (M_\infty^2 - 1)/\tau\lambda M_\infty^2(\gamma + 1) = 0(1) \tag{11}$$

Obviously, K is the generalized transonic parameter for $\lambda = 0(1)$. With Eq. (10) giving the scale factor b'/b for the new region, the requirement for thickness dominance in the nonlinear region $[\alpha \ll \tau r \ln(\varepsilon r)]$, referring to Eq. (6), becomes

$$\sigma \equiv [\alpha/(\tau)^{1/2}]\lambda^{3/2} \ll 1 \tag{12}$$

Next, we consider the other alternative wherein the lift dominates over, or is at least as contributive as, the thickness for some large r. This requires $\tau r \ln \varepsilon r = 0(\alpha)$ or smaller, according to Eq. (6). The perturbation potential may in this case be estimated from Eq. (6) for such a large r as $\varphi/Ub = 0(\alpha/r)$. The order of the error of the inner solution to φ/Ub at large r may then be determined in the same manner as in the preceeding case as

$$R = 0[(M_\infty^2 - 1)\alpha\lambda^2 r + (\gamma + 1)M_\infty^2\alpha^2\lambda^3] \tag{13}$$

Comparison of R with φ/Ub locates the nonuniformity region in this case at

$$r = 0(b'/b) = 0(1/\alpha\lambda^3) \tag{14}$$

where $\varphi/Ub = 0(\alpha^2\lambda^3)$, provided

$$K/\sigma^2 = 0(1) \tag{15}$$

The requirement for the lift dominance in the nonlinear region [i.e., $\tau r \ln(\varepsilon r) \ll \alpha$] now becomes

$$\sigma \gg 1 \tag{16}$$

The foregoing examination has uncovered three domains of the transonic small disturbance regime for $\lambda = 0(1)$ controlled by the ratio $\alpha\lambda^3/(\tau\lambda^3)^{1/2}$, i.e., by $\sigma \equiv \alpha\lambda^{3/2}\tau^{-1/2}$,

a) $\sigma \ll 1$, (thickness dominated)

b) $\sigma = 0(1)$, (intermediate)

c) $\sigma \gg 1$, (lift dominated)

The governing P.D.E. in the outer nonlinear region for each domain is readily obtained after recalling r and φ with the scale factors appropriate to the domain considered.

The Nonlinear Outer Region: Governing Equations

For quite obvious reason, we shall employ the cylindrical polar coordinates for the outer solution. The set of proper scales and new variables for the domain $\sigma \ll 1$ is $x' = x/l$, $\eta = r\{\tau\lambda^3 M_\infty^2(\gamma + 1)\}^{1/2}/b$, $\omega =$ the azimuthal angle, and $\Phi = \varphi/\tau Ub$. The corresponding quantities appropriate to the domain $\sigma \gg 1$ are $x' = x/l$, $\zeta = r\alpha\lambda^3 M_\infty^2(\gamma + 1)/b$, ω and $\Phi = \varphi/\alpha^2\lambda^3 M_\infty^2(\gamma + 1)Ub$. For the (intermediate) domain $\sigma = 0(1)$ either set will suffice.

In the domains $\sigma \ll 1$ and $\sigma = 0(1)$, the reduced P.D.E. for the outer region, dropping the prime in x, is

$$-(K + \Phi_x)\Phi_{xx} + (1/\eta)(\eta\Phi_\eta)_\eta + (1/\eta^2)\Phi_{\omega\omega} = 0 \tag{17}$$

of which the relative error is $0(\tau\lambda)$. Note that the factor $M_\infty^2(\gamma + 1)$ has been absorbed into the scales of η and Φ. As in the plane and axisymmetric cases,[10,11] the conservation form of the P.D.E., obtained readily from Eq. (17) after multiplying both sides by η, admits weak solutions with shock discontinuity surfaces satisfying Rankine-Hugoniot relations subject to a relative error of $0(\tau\lambda)$. In the far field (excluding the vicinity of the axis), we demand

$$\Phi \to 0, \quad \text{as } x^2 + \eta^2 \to \infty \tag{18}$$

In approaching the axis ($\eta \to 0$), we require Φ to match the outer limit of the inner solution Eq. (6). The matching determines $C_1(x)$,ε and $g(x)$ of Eq. (6), and verifies the anticipated relations Eq. (7). As far as the determination of the outer solution is concerned, we only need from Eq. (6) the normal derivative of φ in terms of the outer variables x, η, ω and Φ near the inner limit $\eta \to 0$ (omitting terms of order $S^2\eta \ln \eta$ and $\sigma^2 \ln \eta$)

$$2\pi\eta(\partial\Phi/\partial\eta) \sim \underbrace{dS/dx}_{\text{(source)}} - \underbrace{M_\infty(\gamma + 1)^{1/2}\{\sigma f_j - (\tau\lambda^3)^{1/2}(d/dx)(\bar{x}_j S)\}l_j(\omega)/\eta}_{\text{(doublet)}} \tag{19}$$

Equations (17–19) specify the solution Φ in the nonlinear outer region [for $\sigma = 0(1)$ or smaller]; all variables as well as parameters, except the variables x and η in the inner and outer limits (18) and (19), belong to unit order under the condition Eq. (2).

In terms of the second set of variables cited, we arrive at the system of reduced equations corresponding to Eqs. (17–19) for the domain $\sigma \gg 1$. This equation system is omitted here to

conserve space. In either system, one can clearly see that the configuration geometry and lift control the outer nonlinear region only through the source and doublet distributions at the axis, in the manner described by Eq. (19). In particular, the degree of asymmetry of the outer flow is controlled primarily by σ. In the domain $\sigma \ll 1$, the solution to Eqs. (19–21) approaches an axisymmetric one, bearing out the area rule; but the lift and other asymmetry effects being of the orders $\sigma \equiv \alpha\lambda^{3/2}\tau^{-1/2}$ and $(\tau\lambda^3)^{1/2}$, are not all together negligible for $\lambda = 0(1) \neq 0$ [refer to Eq. (19)]. It is of interest to note from Eq. (19) that even at zero lift, there is a correction proportional to $(\tau\lambda^3)^{1/2}(d/dx)(\bar{x}_j S)$, which is numerically small for most configurations but is appreciable for planforms without bilateral symmetry, such as example c in Fig. 1.[12]

Equivalence Rule and Similitude

Inspection of Eqs. (17–19) for $\sigma \leqq 0(1)$ and the corresponding system for $\sigma \gg 1$ reveals that the similarity parameters, in addition to K, are $M_\infty(\gamma+1)^{1/2}\sigma$ and $M_\infty\{(\gamma+1)\tau\lambda^3\}^{1/2}$. The more important features of the similitude are the equivalence rule implied by Eq. (19) and the corresponding equation for $\sigma \gg 1$. In terms of the variables x, η, ω and Φ, the nonlinear field structure as well as the far-field pattern are invariant so long as K is fixed and the equivalent source and doublet distributions, i.e.,

$$dS/dx \quad \text{and} \quad M_\infty(\gamma+1)^{1/2}\{\sigma f_j - (\tau\lambda^3)^{1/2}(d/dx)(\bar{x}_j S)\} \quad (20)$$

remain the same. This rule requires the same cross-sectional area distribution; the same lateral force distribution is, however, not strictly required when σ and $(\tau\lambda^3)^{1/2}$ are comparable.

Remarks

The frame work of the study outlined above may be defined, instead of Eq. (2), by $|M_\infty - 1| \ll 1$, $(\tau\lambda^3)^{1/2} \ll 1$ and $\alpha\lambda^3 \ll 1$. This may be compared with the requirements in a formulation by Cole[13] for a class of high aspect ratio wings, namely $|M_\infty - 1| \ll 1$, $\tau \ll 1$, $\tau\lambda^3 = 0(1) = \alpha\lambda^3$. Therefore, the present formulation, together with Cole's, encompasses the whole range of λ. However, like the classical slender-body theory[6–8] the present formulation is not directly applicable to rectangular planforms, the vicinity of the straight trailing edge of a flat-plate triangular wing, as well as the neighborhood of any station containing a slope discontinuity in the surface or planform. A fuller development of the theory, with supporting numerical analyses, will appear in subsequent papers. The relations of the present research to other transonic studies (flowfield computation, far-field analysis, critical-wing design, etc.) are discussed in Ref. 14.

References

[1] Whitcomb, R. T., "A Study of the Zero-lift Drag Rise Characteristics of Wing Body Combinations Near the Speed of Sound," RM-L52H08, 1952, NACA.

[2] Oswatitsch, K. and Keune, F., "Ein Äquivalenzsatz für Nichtangestellte Flügel Kleiner Spannweite in Schallnäher Strömung," *Zeitschrift für Flügwissenschaft*, Vol. 3, No. , 1954, pp. 29 46.

[3] Guderley, K. G., *The Theory of Transonic Flow*, Pergamon Press, New York, 1962.

[4] Cole, J. D. and Messiter, A. F., "Expansion Procedures and Similiarity Laws for Transonic Flow, Part. I. Slender Bodies at Zero Incidence," *Zeitschrift für Angewandte Mathematik und Physik*, Vol. 8, 1957, pp. 1–25.

[5] Ashley, H. and Landahl, M., *Aerodynamics of Wings and Bodies*, Addison-Wesley, Reading, Mass., 1965.

[6] Jones, R. T., "Properties of Low-Aspect Ratio Pointed Wings at Speeds Below and Above the Speed of Sound," Rept. 835, 1946, NACA.

[7] Ward, G. N., "Supersonic Flow Past Slender Pointed Bodies," *Quarterly Journal Mechanics and Applied Mathematics*, Vol. 2, Pat. 1, 1949, pp. 75–97.

[8] Adams, M. C. and Sears, W. R., "Slender-Body Theory—Review and Extensions," *Journal of the Aeronautical Sciences*, Vol. 20, No. 2, 1953, pp. 85–98.

[9] Spreiter, J. R. and Stahara, S. S., "Aerodynamics of Slender Bodies and Wing-Body Combinations at $M_\infty = 1$," *AIAA Journal*, Vol. 9, No. 9, Sept. 1971, pp. 1784–1791.

[10] Murman, E. M. and Cole, J. D., "Calculation of Plane Steady Transonic Flows," *AIAA Journal*, Vol. 9, No. 1, Jan. 1971, pp. 114–121.

[11] Krupp, J. A. and Murman, E. M., "The Numerical Calculation of Steady Transonic Flows Past Thin Lifting Airfoils and Slender Bodies," AIAA Paper 71-566, Palo Alto, Calif., 1971.

[12] Jones, R. T., "Reduction of Wave Drag by Antisymmetric Arrangement of Wings and Bodies," *AIAA Journal*, Vol. 10, No. 2, Feb. 1972, pp. 171-176.

[13] Cole, J. D., "Twenty Years of Transonic Flows," Document D1-82-0878, July 1969, Boeing Scientific Research Lab., Seattle, Wash.

[14] Cheng, H. K. and Hafez, M., "On Three Dimensional Structure of Transonic Flows," Rept. USCAE 121, July 1972, Univ. Southern Calif., Aerospace Engineering Dept., Los Angeles, Calif.

Cooled Supersonic Turbulent Boundary Layer Separated by a Forward Facing Step

FRANK W. SPAID*

University of California, Los Angeles, Calif.

Nomenclature

C_f = skin-friction coefficient
C_p = pressure coefficient
$\bar{C}_p$ = free interaction parameter, $\bar{C}_p = C_{f0}{}^{1/2}(M_0^2 - 1)^{-1/4}$
h = step height
M = Mach number
p = pressure
Re = Reynolds number
T = temperature
x = coordinate axis aligned with flow direction, with origin at the step
Δx = x distance measured from the beginning of the interaction
δ = boundary-layer thickness

Subscripts

o = undisturbed flow just upstream of the interaction
p = conditions at the plateau, or first peak in the static pressure distribution
r = conditions corresponding to recovery temperature
w = conditions at the wall

THE objective of the present study was to investigate the effect of wall cooling on separation of a turbulent boundary layer by a forward-facing step in supersonic flow.

Experimental Apparatus and Technique

Experiments were conducted on the nozzle wall of the 3 × 3 in. supersonic wind tunnel of the UCLA Aerodynamics Laboratory, at a nomical Mach number of 2.9. The nozzle block on that side was water-cooled over its entire length. A water-cooled brass model which included an adjustable step formed one of the test section walls.

Model static pressures were measured at 30 locations with the aid of two Scanivalves and a 0–5 psid transducer. Model and nozzle block temperatures were sensed at 13 locations by iron-constantan thermocouples.

Pitot pressure and stagnation temperature surveys of the undisturbed boundary layer on the test section wall were conducted at several locations, for each test condition. Displacement thicknesses were consistent with the assumption that transition

Received March 3, 1972; revision received April 13, 1972. This work was supported by the School of Engineering and Applied Science, and by the Campus Computing Network, University of California, Los Angeles.

Index category: Jets, Wakes, and Viscid-Inviscid Flow Interactions.

* Assistant Professor, School of Engineering and Applied Science. Member AIAA.